Supplementary Table S1. Primer sequences used in qRT-PCR analysis

Gene			Primer sequence (5' → 3')
Human	CXCL9	Forward	GGAGATCACCAGTGTGTGGCT
		Reverse	AGGCACTGCATTGTGGTAGGA
	CXCL10	Forward	AATCGATGCAGTGCTTCCAAGG
		Reverse	GCAGCTGATTTGGTGACCATCATT
	GAPDH	Forward	TGACCCCTTCATTGACCTC
		Reverse	TTCCCGTTCTCAGCCTTG
Mouse	H-2Kk	Forward	ACTGGAGCTGTGGTGGCTTT
		Reverse	CACCAAGTCCACTCCAGGCA
	B2M	Forward	GCTCGGTGACCCTGGTCTTT
		Reverse	CGTAGCAGTTCAGTATGTTCGGCTT
	CXCL9	Forward	TCTGGCTTCCAGAGCCACAC
		Reverse	TCTAGCTCACCAGCAAACAGACA
	CXCL10	Forward	GAGGGCCATAGGGAAGCTTGA
		Reverse	GTGTGTGCGTGGCTTCACTC
	CD274	Forward	TGGCAGGAGAGGAGGACCTT
		Reverse	TGTAGTCCGCACCACCGTAG
	GAPDH	Forward	GGAAAGCTGTGGCGTGATGG
		Reverse	AGCTCTGGGATGACCTTGCC

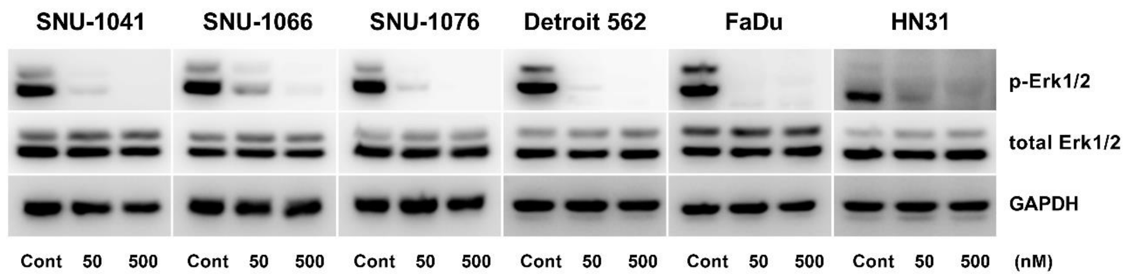

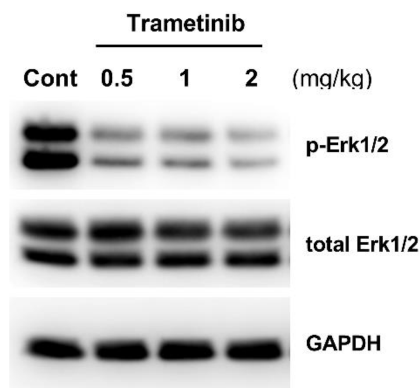

Supplementary Figure S1. Trametinib-induced inhibition of Erk1/2 *in vitro* and *in vivo*. (A) Human HNSCC cell lines were treated with the indicated doses of trametinib. After 24 hours, expression of phospho- and total-Erk1/2 were assessed by Western blotting. Representative images from two independent experiments are shown. (B) Tumor-bearing mice (n=3) received trametinib by oral gavage once daily at the indicated doses. Inhibition of Erk1/2 activation was determined by Western blotting at the endpoint.

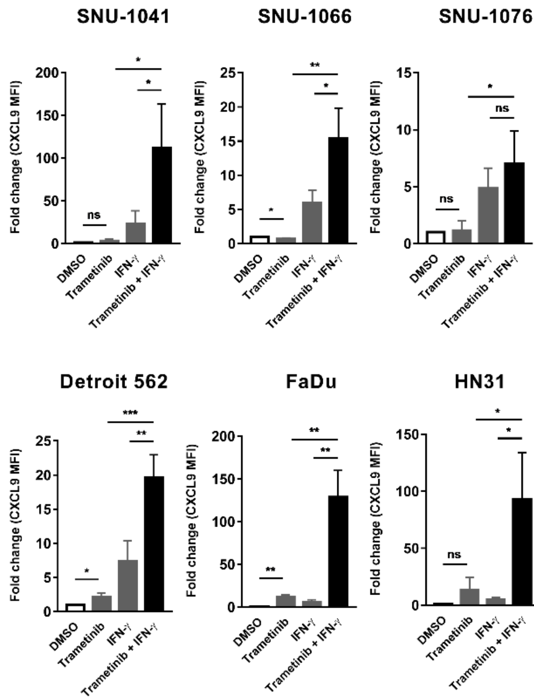
A
SNU-1041
SNU-1066
SNU-1076
Detroit 562
FaDu
HN31
Fold change (CXCL9 MFI)
DMSO
Trametinib
IFN-γ
Trametinib + IFN-γ
ns
*
**
***

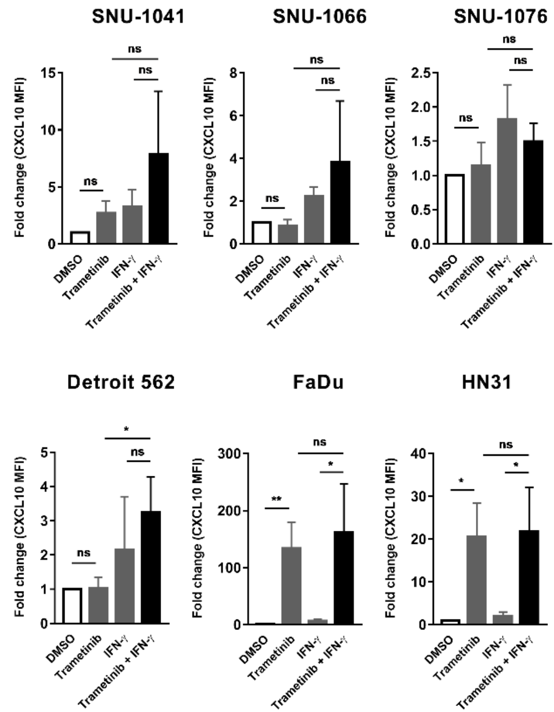
B
SNU-1041
SNU-1066
SNU-1076
Detroit 562
FaDu
HN31
Fold change (CXCL10 MFI)
DMSO
Trametinib
IFN-γ
Trametinib + IFN-γ
ns
*
**

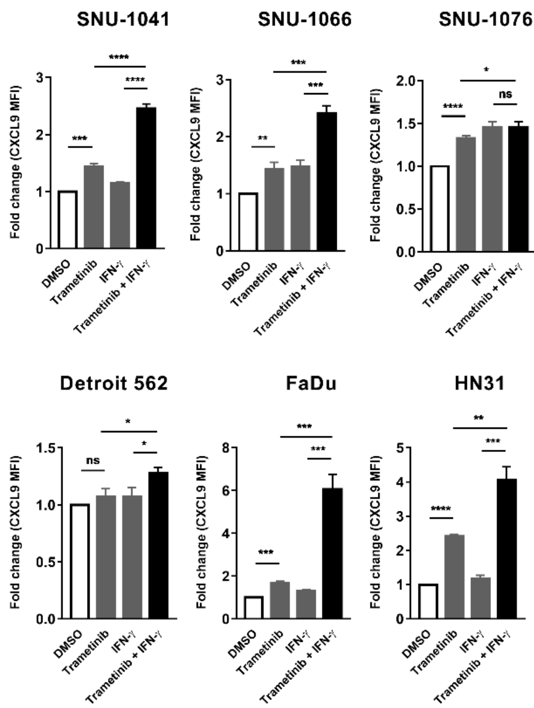
C
SNU-1041
SNU-1066
SNU-1076
Detroit 562
FaDu
HN31
Fold change (CXCL9 MFI)
DMSO
Trametinib
IFN-γ
Trametinib + IFN-γ
ns
*
**
***
****

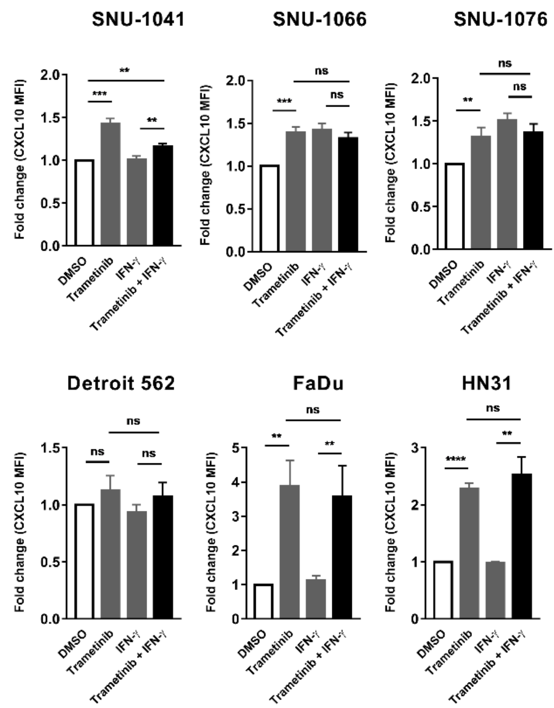
D
SNU-1041
SNU-1066
SNU-1076
Detroit 562
FaDu
HN31
Fold change (CXCL10 MFI)
DMSO
Trametinib
IFN-γ
Trametinib + IFN-γ
ns
**
***
****

Supplementary Figure S2. Trametinib upregulates CXCL9 and CXCL10 protein expression and synergizes with IFN-γ in human HNSCC cell lines. Cells were treated with trametinib (50 nM), IFN-γ (5 ng/ml) or the combination of trametinib and IFN-γ (pretreated with DMSO or trametinib one hour prior to the addition of IFN-γ) for 72 hours. Expression of CXCL9 and CXCL10 were assessed by intracellular flow cytometry. (A and B) The fold change in percentage of cells expressing CXCL9 (A) and CXCL10 (B) was averaged from three independent experiments. (C and D) The fold change in mean fluorescence intensity (MFI) level for CXCL9 (C) and CXCL10 (D) was averaged from three independent experiments. Error bars indicate SD.

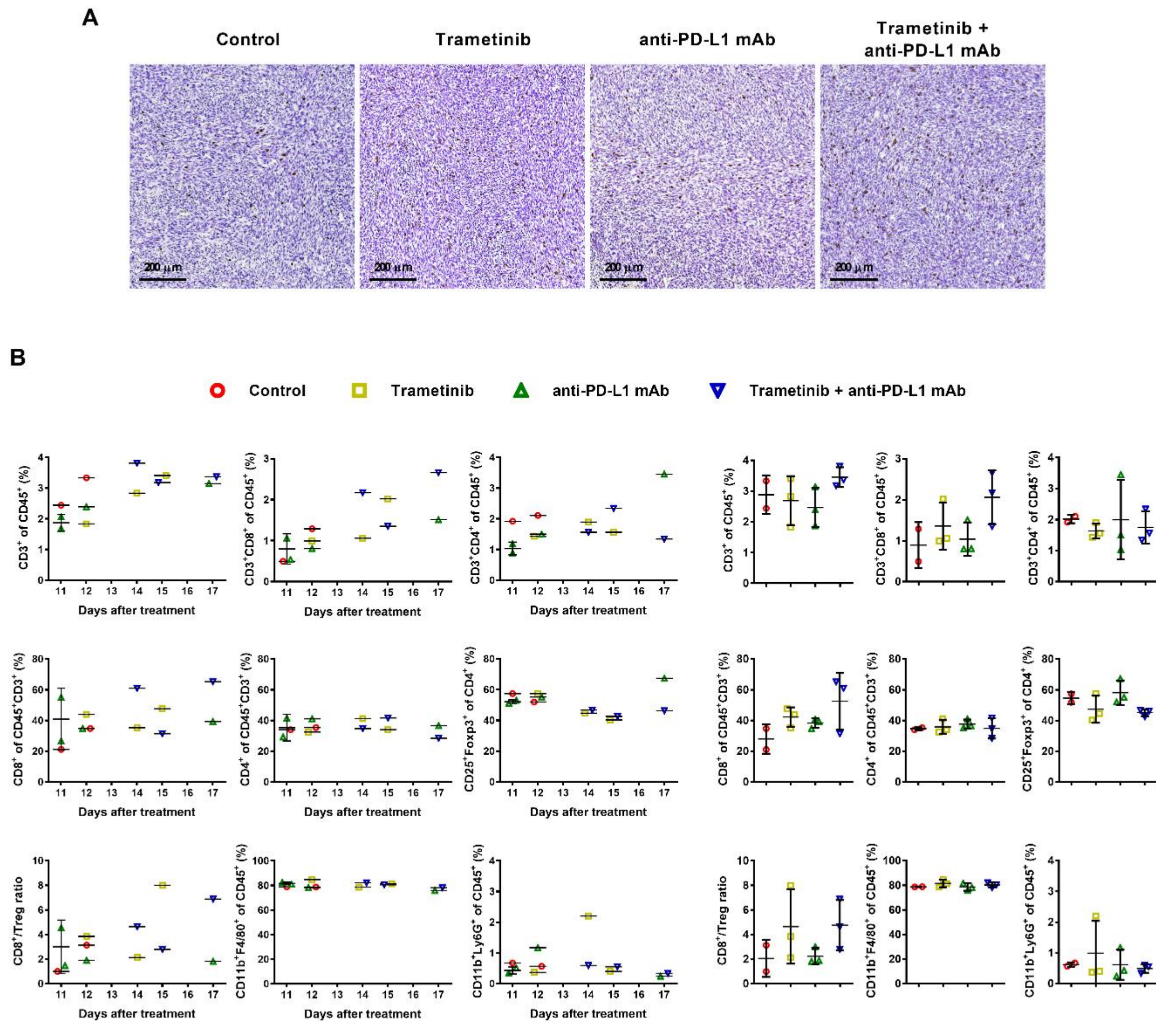

Supplementary Figure S3. Treatment with trametinib and an anti-PD-L1 mAb affects immune composition within the tumor microenvironment. (A) $CD8^+$ T cells within tumor tissues were assessed by IHC staining after five days of treatment (n=3). Scale bar indicates 200 µm. Representative data are shown. (B) Immune cell subsets were analyzed using flow cytometry after gating $CD45^+$ cells at the endpoints (n=2-4). Graphs represent each immune cell subset from individual mice over time (left) and patterns of each group (right).

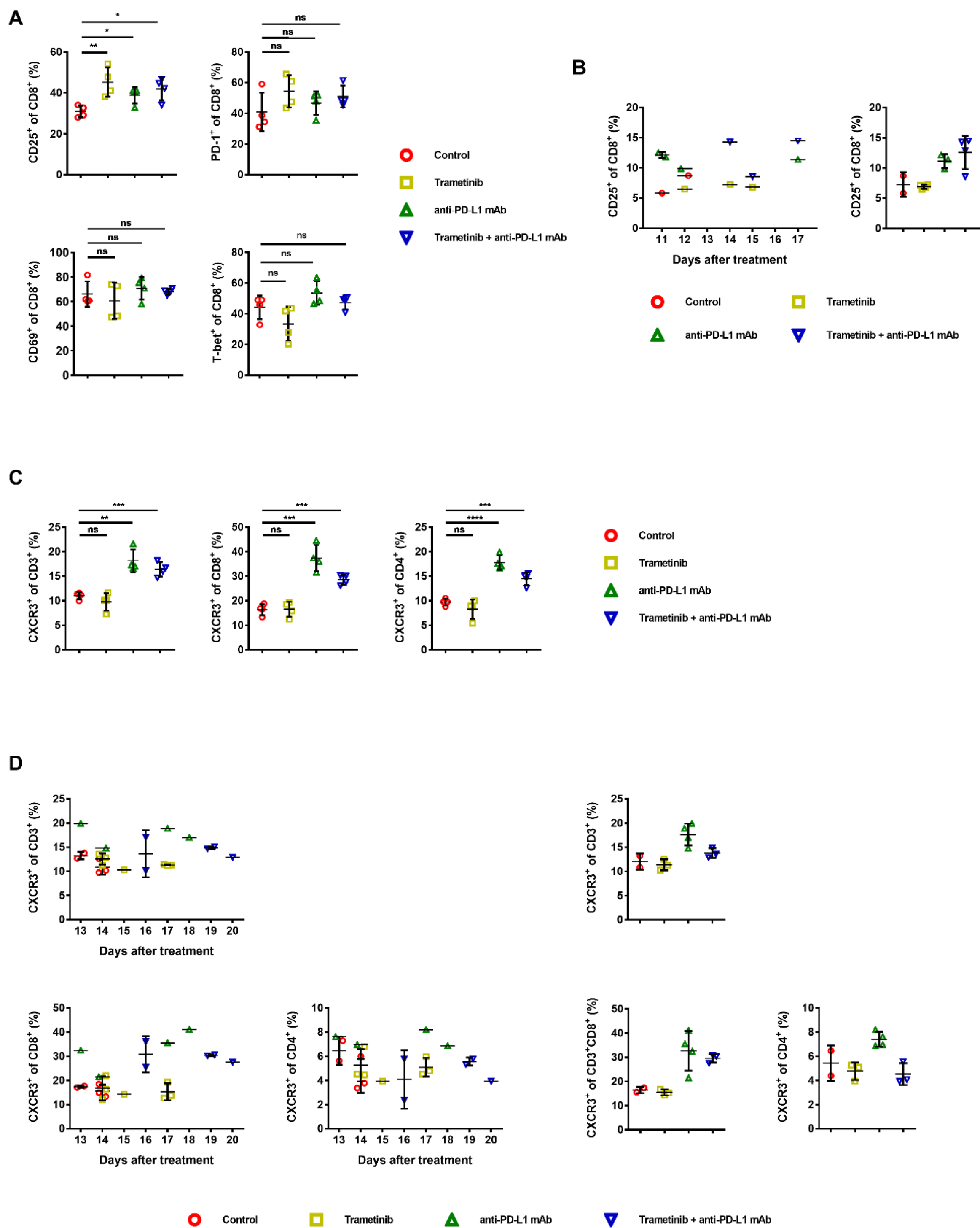

A
CD25+ of CD8+ (%)
PD-1+ of CD8+ (%)
CD69+ of CD8+ (%)
T-bet+ of CD8+ (%)
ns
Control
Trametinib
anti-PD-L1 mAb
Trametinib + anti-PD-L1 mAb
B
CD25+ of CD8+ (%)
Days after treatment
C
CXCR3+ of CD3+ (%)
CXCR3+ of CD8+ (%)
CXCR3+ of CD4+ (%)
D
CXCR3+ of CD3+ (%)
CXCR3+ of CD8+ (%)
CXCR3+ of CD4+ (%)
CXCR3+ of CD3+CD8+ (%)
Days after treatment

Supplementary Figure S4. Trametinib increases CD25 expression within the tumor microenvironment and an anti-PD-L1 mAb enhances CXCR3 expression in splenic T cells. (A and B) Levels of the activation markers including CD25 were measured in tumor-infiltrating $CD8^+$ T cells using flow cytometry after five days of treatment (A) (n=4) and only CD25 at the endpoint (B) (n=2-4) (B) Graphs represent CD25 expression from individual mice over time (left) and patterns of each group (right). (C and D) CXCR3 expression in splenic T cells was analyzed using flow cytometry after five days of treatment (C) (n=4) and at the endpoint (D) (n=4-7; sequential administration of drugs as in Fig. 5E and Supplementary Fig. S7B). (D) Graphs represent CXCR3 expression from individual mice over time (left) and patterns of each group (right).

A

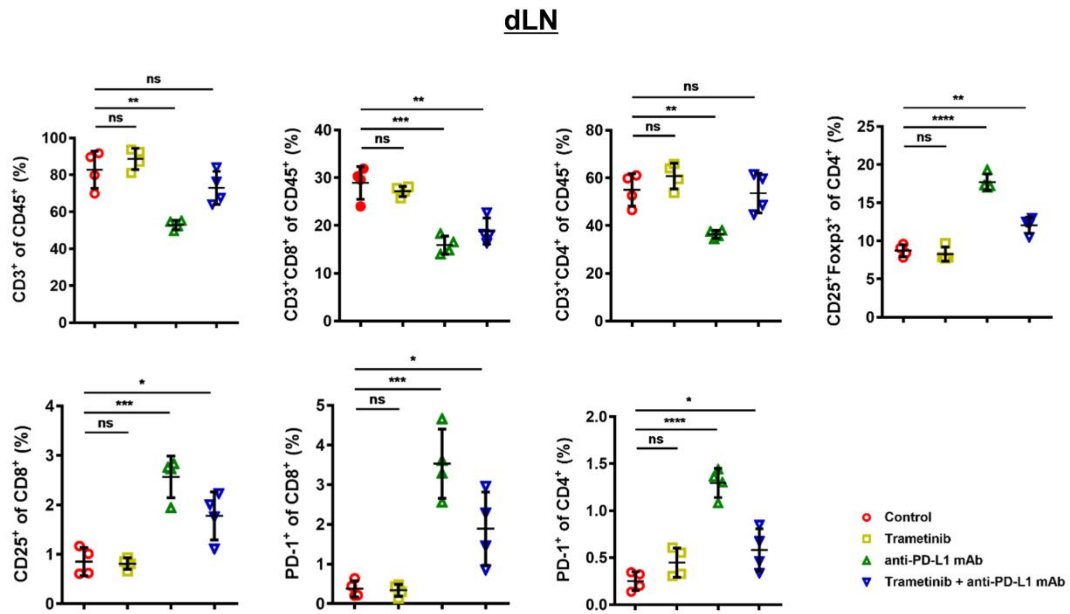

B

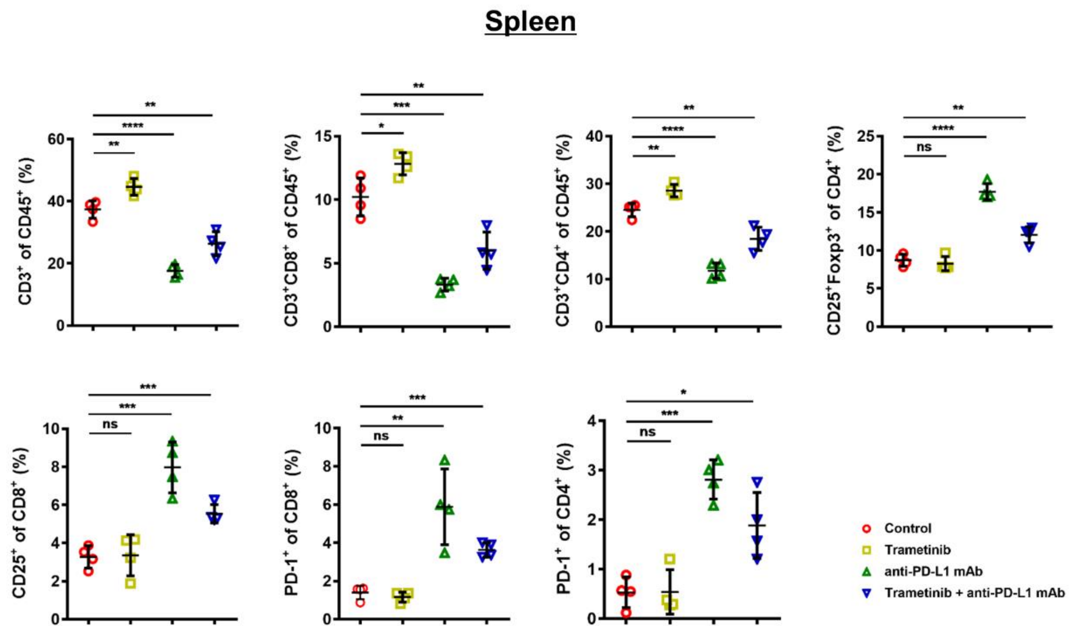

Supplementary Figure S5. The effects of trametinib on T cells were confined to the tumor tissue, whereas the anti-PD-L1 mAb acted systemically. T cell composition and expression of their activation markers within the tumor-draining lymph node (A) and spleen (B) were measured using flow cytometry after five days of treatment.

A

Control

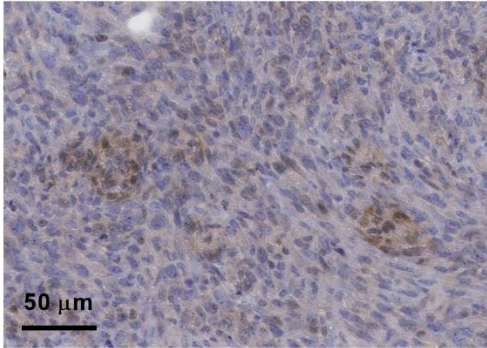

Trametinib

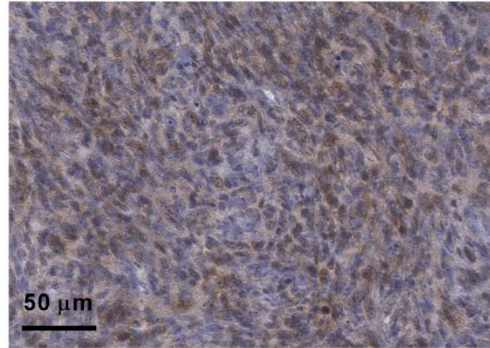

anti-PD-L1 mAb

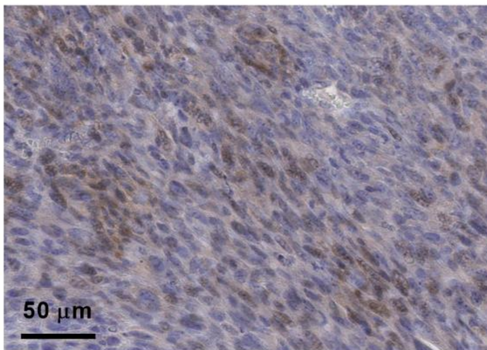

Trametinib + anti-PD-L1 mAb

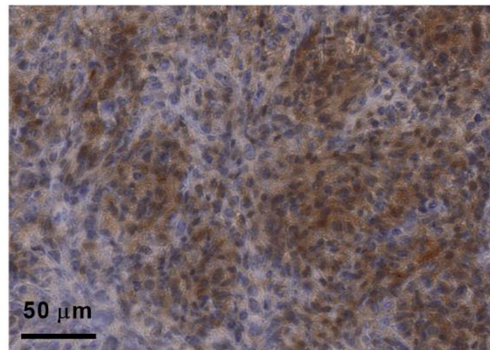

B

1

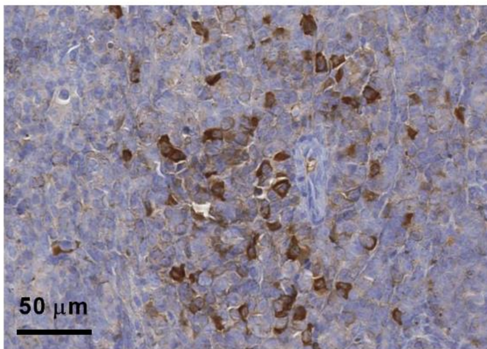

2

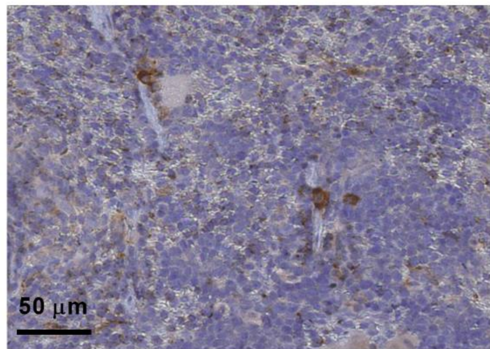

3

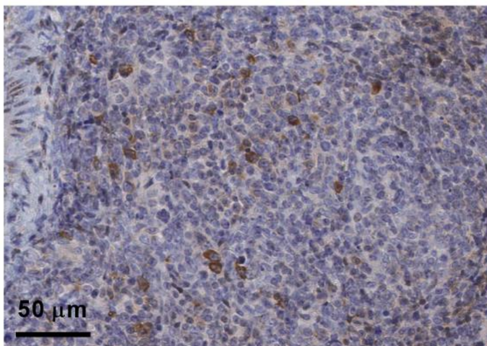

4

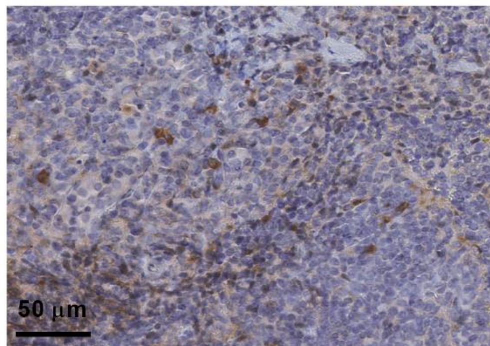

Supplementary Figure S6. Results of PD-L1 immunohistochemistry at 400 X magnification. (A) Higher magnification of PD-L1 IHC shown in Fig. 5D. (B) Staining results of relevant controls. Spleens from naïve (top) and tumor-bearing (bottom) mice were stained with anti-mouse PD-L1 mAb (n=2, respectively). Scale bar indicates 50 μm.

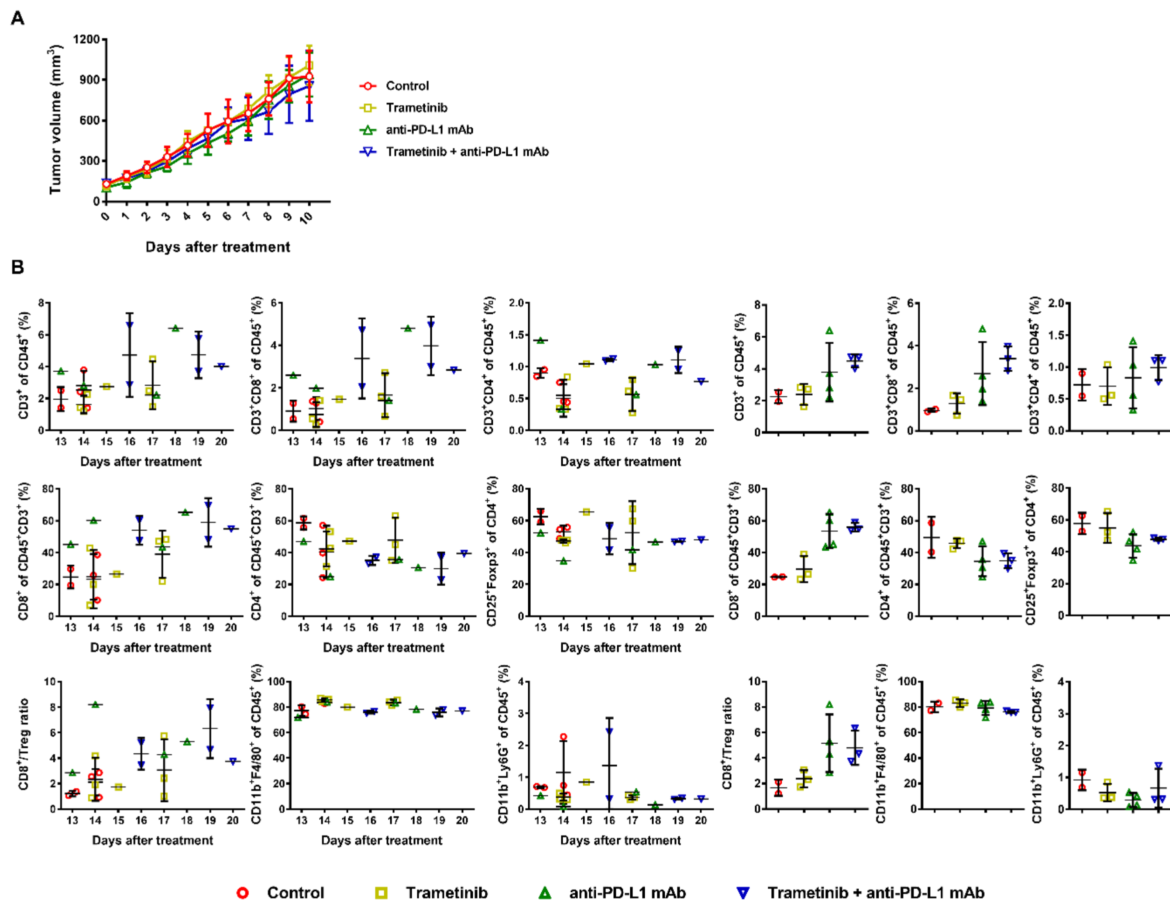

Supplementary Figure S7. Same experiment as in Fig. 5A using BALB/c nude mice and changes in immune cell subset composition with sequential administration of trametinib and an anti-PD-L1 mAb using C3H mice. (A) Tumor-bearing BALB/c nude mice (n=5) were treated with trametinib (1 mg/kg) by oral gavage once daily and/or an anti-PD-L1 mAb (10 mg/kg) by intraperitoneal injection twice weekly. Control mice received vehicle or isotype control. (B) Cells were isolated from tumor tissues (n=4-7) for measuring of each immune cell subset at the endpoints. Graphs represent each immune cell subset from individual mice over time (left) and patterns of each group (right).